A Study on Classification and Localization of Structural Damage through Wavelet Analysis

Bong-Hwan Koh[1], Uk Jung[2]

고봉환(동국대학교 기계공학과), 정욱(동국대학교 경영학과)

Key Words: Damage detection, wavelet transform, silhouette statistics.

ABSTRACT

This study exploits the data discriminating capability of silhouette statistics, which combines wavelet-based vertical energy threshold technique for the purpose of extracting damage-sensitive features and clustering signals of the same class. This threshold technique allows to first obtain a suitable subset of the extracted or modified features of our data, i.e., good predictor sets should contain features that are strongly correlated to the characteristics of the data without considering the classification method used, although each of these features should be as uncorrelated with each other as possible. The silhouette statistics have been used to assess the quality of clustering by measuring how well an object is assigned to its corresponding cluster. We use this concept for the discriminant power function used in this paper. The simulation results of damage detection in a truss structure show that the approach proposed in this study can be successfully applied for locating both open- and breathing-type damage even in the presence of a considerable amount of process and measurement noise.

1. Introduction

This paper investigates a structural damage localization problem using a wavelet-based signal classification method that extracts signal features with the best discrimination ability when classifying the location of stiffness damage in a planar truss structure. The proposed approach uses simulation data generated from a truss model subjected to an unknown random excitation. Since most signal features in the damage-induced response are irrelevant to the class distinction and inevitably corrupted with measurement noises, we first attempt to apply the VET criteria previously proposed by Jung et al. [1]. According to these criteria, good predictor sets should contain features that are strongly correlated to the class distinction, although each of these features should be as uncorrelated with each other as possible; we thus select differentiated features for data dimensionality reduction and noise removal. Secondly, the proposed VETS (VET wavelet positions containing large silhouette statistics) comprises a few features with highest silhouette statistics to find the smaller number of features having more discriminating power for localizing a stiffness-damaged element in a truss structure.

2. Review of Related Theories

2.1 Wavelet Transformation

Discrete wavelet transform (DWT) effectively projects a temporal signal into a special wavelet basis that entails adjustable multiresolution parameters such as scale and position to represent a nonstationary signal. Typically, DWT is performed on multiple levels with different frequency resolutions. As each level of the transformation is performed, there is a trade-off between the time and frequency resolution. The full DWT for a time domain signal in L_2 (finite energy), $f(t)$, can be represented in terms of a shifted version of a scaling function $\phi(t)$ and a shifted and dilated version of a so-called mother wavelet function $\psi(t)$. DWT can be represented as

$$f(t) = \sum_{k \in Z} c_{L,k} \phi_{L,k}(t) + \sum_{j \geq L} \sum_{k \in Z} d_{j,k} \psi_{j,k}(t) \qquad (1)$$

where $d_{j,k}$ are the wavelet coefficients and $c_{L,k}$, $L < J$ are the scaling coefficients. These coefficients are given by the inner product in L_2, i.e.,

$$c_{L,k} = <f(t), \phi_{L,k}(t)> \text{ and } d_{j,k} = <f(t), \psi_{j,k}> . \qquad (2)$$

Here, $\phi_{L,k}(t) = 2^{L/2} \phi(2^L t - k); k \in Z$ is a family of scalar functions and $\psi_{j,k}(t) = 2^{j/2} \psi(2^j t - k); j \geq L, k \in Z$ is a family of wavelet functions. If the mother functions are properly selected, their family forms an orthogonal basis for the signal space.

Consider a sequence of data $\mathbf{y} = (y(t_1), \cdots, y(t_N))$ taken from $f(t)$ or obtained as a realization of $y(t) = f(t) + \varepsilon_t$ at equally spaced discrete time points $t = t_i$ s, where ε_{t_i} s are independent and identically distributed (i.i.d.) noises following $N(0, \sigma^2)$. The discrete wavelet transform (DWT) of $\mathbf{y}$ is defined as $\mathbf{d} = W\mathbf{y}$, where W is the orthonormal $N \times N$ DWT matrix. It is given that $\mathbf{d} = (\mathbf{c}_L, \mathbf{d}_L, \mathbf{d}_{L+1}, \cdots, \mathbf{d}_J)$, where $\mathbf{c}_L = (c_{L,0}, \cdots, c_{L,2^L-1})$, $\mathbf{d}_L = (d_{L,0}, \cdots, d_{L,2^L-1})$, and $\mathbf{d}_J = (d_{J,0}, \cdots, d_{J,2^J-1})$.

754

Using inverse DWT, the $N \times 1$ vector $\mathbf{y}$ of the original signal curve can be reconstructed as $\mathbf{y} = W^T \mathbf{d}$. By applying DWT to the data $\mathbf{y}$ s, $\mathbf{d} = W\mathbf{y}$, we obtain the following model in the wavelet domain: $d_{j,k} = \theta_{j,k} + \eta_{j,k}$ for $j = L, \cdots, J$, $k = 0, 1, \cdots, 2^j - 1$, and $c_{L,k} = \theta_{L,k} + \eta_{L,k}$ for $k = 0, 1, \cdots, 2^L - 1$, where $J = \log_2 N - 1$. The model can be represented in the vector format as follows.

$$\mathbf{d} = \theta + \eta \qquad (3)$$

where $\mathbf{d}, \theta$, and η represent the collection of all coefficients, parameters, and errors, respectively. Since W is an orthonormal transform, $\eta_{j,k}$'s are still i.i.d. $N(0, \sigma^2)$ [6]. In order to simplify the notation used in this paper, $\mathbf{d} = (d_1, d_2, \ldots, d_N)$ is used instead of c_{Lk} and d_{jk} for the components of $\mathbf{d}$.

2.2 Wavelet Model for Multiple Signals

We denote a vector of N equally-spaced data points from a signal curve, where $N = 2^J$ with some positive integer J and $i = 1, 2, \cdots, M$ by $y_i = [y_{i1}, y_{i2}, \cdots, y_{iN}]$. Let $Y = [y_1, y_2, \cdots, y_M]^T$ be the collection of M multiple sets of functional data. When DWT W is applied to a data set, the matrix of wavelet coefficients obtained from this transformation is $D = WY$, where $D = [d_1, d_2, \cdots, d_M]^T$, $d_i = [d_{i1}, d_{i2}, \cdots, d_{iN}]$, and d_{im} is the wavelet coefficient at the mth wavelet position for the ith data curve. The model of wavelet coefficients D from M signals is given as follows:

$$D = \Theta + Z \qquad (4)$$

where $\Theta = [\theta_1, \cdots, \theta_M]^T$ ($\theta_i = [\theta_{i1}, \theta_{i2}, \cdots, \theta_{iN},]$) and Z is a column of $M \times N$ random errors with normal distribution $N(0, \sigma^2)$. The measurement error (noise) variation of the wavelet coefficients is characterized by the common process variance σ^2 for multiple signals.

3. Data Classification Methodology

3.1 Data Pre-selection by Vertical Energy Threshold (VET)

Most wavelet-related models for analyzing complicated signals have focused on feature selection and noise removal for the case of a single signal. However, many engineering applications require the simultaneous processing of multiple signals to understand the nature of a system or to extract

hidden features of the defects within the system. Although a method for single-signal-based wavelet feature selection can be applied to process multiple signals, it can cause a problem in that different numbers and choices of representative wavelet features in different signals constitute no "unified wavelet-positions" in the comparison of signals, especially in the case of signals from different classes in a distinct process effect. Therefore, Jung et al. used the advantages afforded by scalograms [2] and developed the following VET procedure [1]. This wavelet feature selection procedure balances the reconstruction error against the data-reduction efficiency and proves that is powerful at capturing key patterns in multiple signals while removing the embedded noise. The selected wavelet coefficients are treated as the "reduced-size" data (reduced number of features) in subsequent analysis for decision making such as clustering and classification. The study introduced the overall relative reconstruction error ($ORRE$) function for processing multiple signals as follows:

$$ORRE(\lambda) = \Lambda(\lambda) + \xi \cdot \Upsilon(\lambda) \qquad (5)$$

where

$$\Lambda(\lambda) = \frac{\sum_{m=1}^{N} E[\| d_{vm}(1 - I(\| d_{vm} \|^2 > \lambda)) \|^2]}{\sum_{m=1}^{N} E[\| d_{vm} \|^2]} \qquad (6)$$

$$\Upsilon(\lambda) = \frac{\sum_{m=1}^{N} E[I(\| d_{vm} \|^2 > \lambda)]}{N}. \qquad (7)$$

Here, E represents the expectation of random variables. Note that equations (6) and (7) include the indicator function, $I(\| d_{vm} \|^2 > \lambda)$, which constitutes the threshold parameter. The indicator function is based on the "vertical energy" metric,

$$\| d_{vm} \|^2 = d_{1m}^2 + d_{2m}^2 + \ldots + d_{Mm}^2, \quad m = 1, 2, \ldots, N, \qquad (8)$$

which is the sum of all wavelet coefficients at the mth wavelet position. This is why it is called vertical-energy-based threshold (VET). Further, the $ORRE$ criterion was originally developed due to the requirement for balancing the reconstruction error and the data-reduction ratio. Equation (6) represents a "normalized" reconstruction error from the wavelet approximation model $Y = W^T D$. On the other hand, equation (7) indicates the number of normalized wavelet coefficients. This term is used as a penalty for including an excessive number of wavelet coefficients so that the data model can be approximated and represented in the simplest manner possible. Normally, the weighting parameter of the penalty, ξ, in equation (5) should be

defined by the user. Alternatively, it can be provided by the generalized cross validation (GCV) method [3]. For simplicity, this study assumes $\xi = 1$, which places equal weights on both components, Λ and Υ.

Given VET in equation (8), *ORRE* is minimized to determine λ. Therefore, a simple formula for estimating the optimal λ with $\lambda_{N,M}$ is developed as

$$\lambda_{NM} = \sum_{m=1}^{N} E(\| d_{vm} \|^2)/N. \qquad (9)$$

Since every wavelet coefficient is independent and has a normal distribution, the vertical energy of each wavelet position follows a non-central chi-square distribution [4]. Based on this result and some other calculus derivations, Jung et al. [1] proved the optimality of λ_{NM}. Therefore, the ith position of the wavelet coefficients (across signals) can be selected if its vertical energy is larger than $\lambda_{N,M}$.

3.2 Discriminant Analysis through Silhouette Statistics

This section describes a new approach for feature selection that generates VETS. Silhouette statistics have been widely used to assess the quality of clustering by measuring how well an object is assigned to its corresponding cluster. See reference [2] for more details on silhouette statistics. Here, this concept is expanded to the discriminant power function, as shown in equation (10) below. For signal pattern classification, it is assumed that a data set is given in which $H = (\vec{d_j}, G(j))$ for $j = 1, \cdots, M$. The data set has M data points with well-defined class labels. Note that $\vec{d_j} = (d_{1j}, d_{2j}, \cdots, d_{pj})$ is the signal vector for the jth sample described by p predictor variables that are pre-selected by VET (where $p = \sum_{m=1}^{N} I(\| d_{vm} \|^2 > \lambda_{NM})$), i.e., the number of wavelet positions selected by the VET procedure) and $G(j) \in G = \{G_1, G_2, \cdots, G_k\}$ is the class label associated with $\vec{d_j}$. Note also that k is the number of classes and n_k is the number of $\vec{d_j}$ in G_k. The proposed discriminant power function based on silhouette statistics at the ith VET feature is then defined as

$$S_i = \frac{1}{M} \sum_{i=1}^{M} \frac{b_i(\vec{d_j}) - a_i(\vec{d_j})}{max\{a_i(\vec{d_j}), b_i(\vec{d_j})\}}, \quad i = 1, 2, \cdots, p \qquad (10)$$

where, for $\vec{d_j} \in G_k$,

$$a_i(\vec{d_j}) = \frac{1}{n_k - 1} \sum_{\vec{d_{j'}} \in G_k} d_i(\vec{d_j}, \vec{d_{j'}}) \qquad (11)$$

$$b_i(\vec{d_j}) = \min_{s \neq k} \frac{1}{n_k} \sum_{\vec{d_{j'}} \in G_s} d_i(\vec{d_j}, \vec{d_{j'}}). \qquad (12)$$

and

$$d_i(\vec{d_j}, \vec{d_{j'}}) = (d_{ij} - d_{ij'})^2 \qquad (13)$$

In other words, $a_i(\vec{d_j})$ is the average distance between $\vec{d_j}$ and all other samples in the same class with respect to the ith wavelet position and $b_i(\vec{d_j})$ is the minimum average distance of $\vec{d_j}$ to all samples in other classes with respect to the ith wavelet position. The discriminant power function with respect to the ith wavelet position, S_i, returns a discriminant power score in the range of -1 to $+1$, and indicates how well all data points can be assigned to their own class in terms of the ith wavelet position. Intuitively, data points are well-classified by wavelet positions with a large silhouette statistic value, data tend to lie between classes with small silhouette values, and data points are poorly classified by those with negative values. According to the perspective of the silhouette statistics, this study will utilize S_i to select a few important wavelet positions for further cluster visualization and classification analysis, i.e., sorting the mean silhouette statistics (discriminating power function) in ascending order:

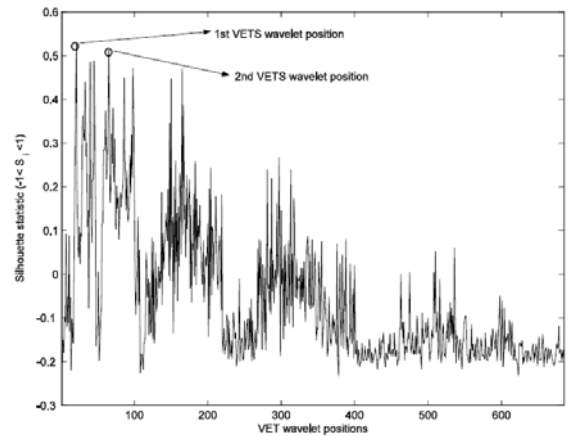$$S_{(1)} < S_{(2)} < \cdots < S_{(p)}, \quad p = \sum_{m=1}^{N} I(\| d_{vm} \|^2 > \lambda_{NM}) \qquad (14)$$

Figure 1. Silhouette statitics of 685 VET wavelet positions

Figure 1 shows the silhouette statistics, S_i, $i = 1, \cdots, p$ ($p = 685$ in this simulation) for each VET wavelet position. The largest silhouette statistics S_i (= 0.5260) leads us to select the first VETS wavelet position (1st VETS

wavelet position = 38th VET wavelet position = $d_{8,6}$), the second largest S_i (= 0.5136) to the second position (2nd VETS wavelet position = 85th VET wavelet position = $d_{7,21}$), and so on.

4. Description of Simulations

4.1 Damage in Truss Structure

The physical system is an eight-bay planar truss structure, as shown in Figure 2. The truss structure is 4-m-long and has two cross-braces in each bay. All truss members comprise an aluminium solid bar whose Young's modulus (E) is $70 \times 10^9 N/m$. Each strut is $2\,cm$ in diameter and the length of each bay is $0.5\,m$. Its boundary condition is shown as a cantilevered truss that is fixed on a solid wall to the left. In order to extract the dynamics of the system, Gaussian random noise input applies as an excitation force at point A as shown in the figure. The response of the system, i.e., the end displacement of point S along the direction of the arrow is collected as time-history data.

Here, we investigate two different types of damage. The first one is an open-type (slot) crack, implying that no stiffness variation occurs as the member experiences compression and expansion. In other words, the strut will have the same bending stiffness although the member undergoes compression (crack closure) and expansion (crack opening). On the other hand, a structure having a breathing-type (fatigue) crack typically behaves as a bilinear system, where the bending stiffness instantaneously changes between two states, i.e., undamaged and damaged.
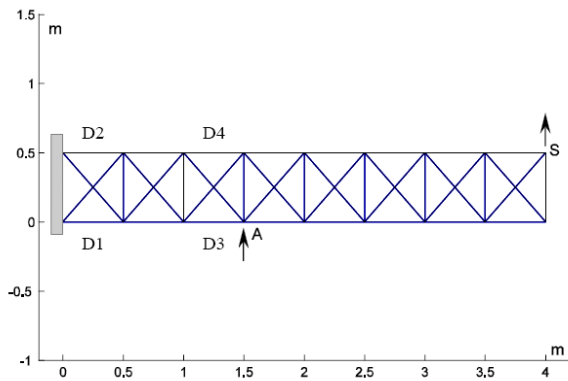

Figure 2. Schematics of an eight-bay planar truss structure with possible damage locations (D1~D4), displacement sensor location (S), and actuator location (A).

Figure 2 also indicates four possible damage locations (D1 ∼ D4), which will be eventually localized through the proposed wavelet-based algorithm. In order to simulate structural defects or damage, the bending stiffness (EI) of the beam element is reduced by 50% in elements D1 through D4 (i.e., 1.0 for healthy and 0.5 for damaged state). For comparative study, the dynamic behaviour of two

damage types, i.e., open- and breathing-type crack is also realized in this simulation. In order to accommodate breathing-type damage, a pair-comparison between two nodes of damaged beam elements is performed at each time step. According to the result of the current time step, i.e., the sign of the relative displacement between adjacent nodes, the elemental stiffness matrix is switched to a stiffness-reduced one for the analysis of the next time step. In other words, the compression and expansion modes of the damaged strut member alternate between different stiffness matrices in each time step. Consequently, nine scenarios are investigated, i.e., four damage location cases for two different damage types and one healthy case.

4.2 Characteristics of Simulation Data

The simulation generates sampled data at the rate of 1000 Hz for 20 s resulting in $N = 20,000$ data points. In order to facilitate uncertainties in the severity of damage, the level of reduced bending stiffness on the damaged truss member is randomly perturbed from its mean value. Therefore, the simulation is repeated 10 times to create a group of randomly populated data sets for all healthy and damaged cases, i.e., the data model of this simulation can be written as

$$y_i = \mathbf{f}(t; \beta_i) + \mathbf{e}^{(\mathbf{n})}, \ \beta_i = g(a_i, b_i, \gamma_i, \rho_i) \qquad (15)$$

where $y_i = [y_{i1}, y_{i2}, \cdots, y_{iN}]$ is a vector of N equally-spaced data points from the ith signal (i = 1,2,…,10); $\mathbf{e}^{(\mathbf{n})} \dfrac{-b \pm \sqrt{b^2 - 4ac}}{2a}$, a vector of random noise; and β_i, a signal-specific parameter for the ith signal. While this variation in damage severity attempts to mimic unforeseen influences in the process error, a white noise ($\mathbf{e}^{(\mathbf{n})}$) is additionally imposed on each time-history data set to create measurement noise. $y_{ij} = f(t_j; \beta_i) + \varepsilon_j^{(n)}$ can be used in other expressions. In the above model, $g(\cdot)$ is an unknown function of parameters such as damage location a_i, damage severity b_i, perturbation level of damage severity γ_i, and type of damage ρ_i, i.e., open or breathing crack. The damage location parameter a_i is defined as

$$a_i \in A = \{0, 1, 2, 3, 4\} \qquad (16)$$

where $a_i = 0$ indicates that the ith signal is from an undamaged (healthy) case. Similarly, if $a_i = 1, 2, 3,$ and 4, the signals are those arising from the damaged cases at locations D1, D2, D3, and D4, respectively. b_i and γ_i are defined as

$$b_i = b + \varepsilon_i^{(b)}, \quad \varepsilon_i^{(b)} \sim N(0,(k \cdot b/3)^2) \tag{17}$$

where

$$b = \begin{cases} 1 & if \quad a_i = 0 \\ 0.5 & otherwise. \end{cases}$$

$$k = \begin{cases} 0 & if \quad a_i = 0 \\ \gamma_i & otherwise. \end{cases} \tag{18}$$

$$\gamma_i \in \Gamma = \{0.1, 0.05, 0.01\}.$$

In the definition above, $\varepsilon_i^{(b)}$ is a realization of damage severity perturbation, i.e., if the signal is from a healthy case ($a_i = 0$), there is neither damage severity nor perturbation of damage severity. Unless the signal is from a healthy case, $\varepsilon_i^{(b)}$ has some value of damage severity perturbation with a parameter γ_i. Here, the value of γ_i is assumed as $Pr(-\gamma_i \cdot b < \varepsilon_i^{(b)} < \gamma_i \cdot b) = 2(\Phi(3) - 0.5) = 0.997$, where $\Phi(z) = \int_{-\infty}^{z} \frac{1}{\sqrt{2\pi}} e^{-\frac{x^2}{2}} dx$. With regard to the damage type, $\rho_i = 0$ for an open crack case while $\rho_i = f(t_j; y_{ij}(t))$ for a breathing crack, which results in the bilinear dynamic behaviour described in the previous section.

As mentioned above, all signals of each damage case include randomly perturbed damage severity (in this figure, $\gamma_i = 0.1$). The signal-to-noise ratio (SNR) is defined as $std(f)/\sigma$, where $std(f)$ is the standard deviation of the discretized signal points and σ is the standard deviation of noise. In the data model, the realization of measurement errors $\varepsilon_j^{(n)}$ is defined as

$$\varepsilon_j^{(n)} \sim N(0, (\frac{std(\mathbf{f}(\mathbf{t}; a_i = 0))}{SNR})^2) \tag{19}$$

where $std(\mathbf{f}(\mathbf{t}; a_i = 0))$ is the standard deviation of the signal from the healthy case.

5. Damage Localization Results

5.1 Clustering Analysis using VETS

Simulation studies are conducted for two different damage types (open- and breathing-type cracks), three values of damage severity variation parameters ($\gamma_i \in \Gamma = \{0.1, 0.05, 0.01\}$), and three SNR levels (7, 5, and 3) on $\mathbf{e}^{(n)}$. The signal from a damaged case with large γ_i and small SNR inherently exhibits more variable and noisier signals in a class. Therefore, 18 different simulation cases are generated. Furthermore, these cases are created for each different damage condition, i.e., four different damage locations, respectively. Note that only three SNR cases are considered for the healthy condition.
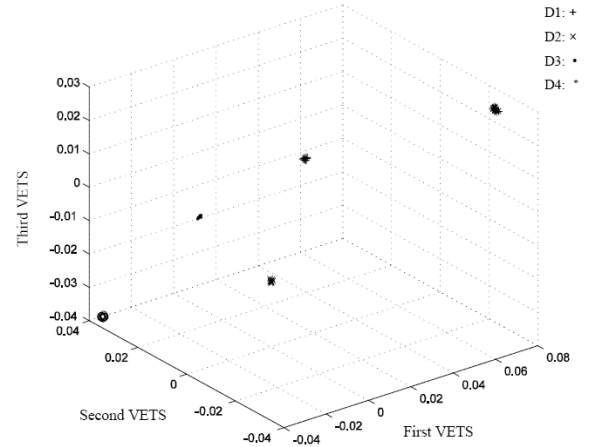

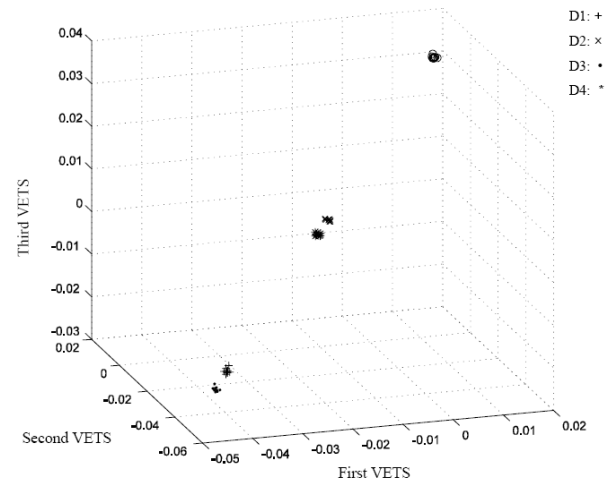Figure 3. VETS clustering for the open crack with and $\gamma = 0.01$ and $SNR = 7$.

Figure 4. VETS clustering for the breathing crack with and $\gamma = 0.01$ and $SNR = 7$.

This study shows a few representative cases with the most variable simulation setting ($\gamma = 0.1$ and $SNR = 3$) and the least variable one ($\gamma = 0.01$ and SNR) for both open and breathing damage cases. Figures 7 through 10 show some of the results from the clustering analysis for damage classification using the VETS wavelet positions. The goal of VETS-based clustering is to discriminate the existence, type, and location of damage in a truss structure. Here, the first three VETS wavelet positions are used for extracting damage-sensitive features for clustering. As shown in Figure 3, four different damage locations, i.e., D1~D4 along with the healthy case are clearly localized in a group when they are projected to the first three VETS wavelet positions. Obviously, the damage locations in the

breathing-type damage cases (Figure 4) are less distinct than those in the open-type ones (Figure 3) under the same perturbation parameter and SNR. This trend becomes more significant as γ increases and SNR decreases, as shown in Figures 5 and 6. With regard to an extreme case, the largest process perturbation $\gamma = 0.1$ and the lowest $SNR = 3$ in conjunction with breathing-type damage produced the worst discrimination result, as shown in Figure 6. However, all 50 signals generated from the four different damage locations and one healthy condition (ten for each condition) have been sufficiently separated and well clustered overall for both open- and breathing-type damage. One can predict that as γ increases above 0.1, i.e., the uncertainty of damage severity increases, the size of the VETS cluster will also increase. This trend can be used to statistically determine the confidence level of a damage location.
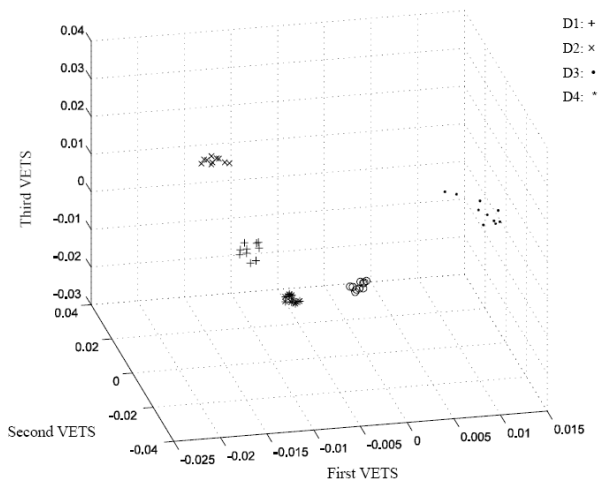

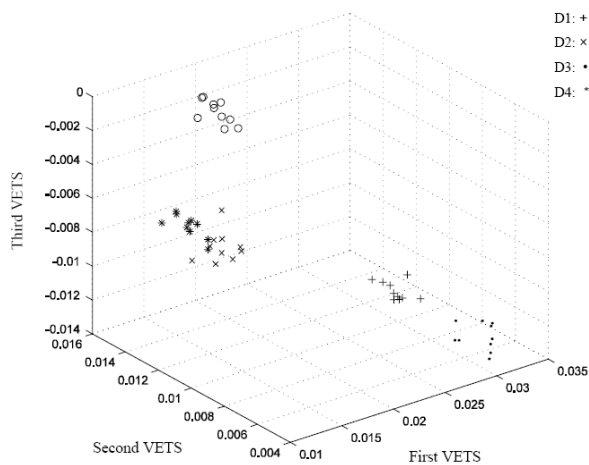Figure 5. VETS clustering for the open crack with and $\gamma = 0.1$ and $SNR = 3$.

Figure 6. VETS clustering for the breathing crack with and $\gamma = 0.1$ and $SNR = 3$.

6. Conclusions

This study uses an eight-bay planar truss structure to validate the proposed damage localization method. Two different types of damage, i.e., open and breathing conditions are investigated to test the benefits of wavelet-based signal processing. The simulated time history responses are processed to extract damage-sensitive wavelet positions, which are further developed to classify damage locations by exploiting VETS-based clustering analysis. The simulation results showed that the proposed approach successfully classified and localized the locations of stiffness-reduced damage in a truss structure even with a significant amount of noise and damage severity uncertainties.

References

[1] Jung, U., Jeong, M. K., and Lu, J, C., "A vertical-energy-thresholding procedure for data reduction with multiple complex curves," *IEEE Transactions on Systems, Man, and Cybernetics-Part B*, 36(5), pp. 1128–1138, 2006.

[2] Rousseeuw, P.J., "Silhouettes: a graphical aid to the interpretations and validation of cluster analysis," *Journal of Computational and Applied Mathematics*, Vol. 20, pp. 53–65, 1987.

[3] Weyrich, N., and Warhola, G.T., "Wavelet shrinkage and generalized cross validation for image denoising," *IEEE Trans. Image Process.*, Vol. 7, No. 1, pp. 82–90, 1998.

[4] Johnson, N.L., and Kotz, S., (1970) *Continuous Univariate Distributions*, Vol. 2, Houghton-Mifflin.